Supplementary Information

Low frequency stimulation induces polarization-based capturing between normal, cancerous and white blood cells; A new separation method for circulating tumor cells enrichment or phenotypic cell sorting

Authors

Mojtaba Jahangiri [1], Mina Ranjbar-Torkamani [1], Hadi Ghafari [1], Hamed Abadijoo [1], Mohammadreza Ghaderi Nia [1], Amir Mamdouh [1], Mohammad Abdolahad [1, C]

[1] Nano Electronic Center of Excellence, Nano Bio Electronics Laboratory, School of Electrical and Computer Engineering, College of Engineering, University of Tehran, 14395/515, Tehran, Iran;

[C] *Corresponding Author;*

Corresponding email: m.abdolahad@ut.ac.ir

- **Laminarity verification by Reynolds Number (Re):**

Laminarity in flow is measured by the Reynolds number (Re): [1][2]

Re < 2300 (laminar)
2300 < Re < 2900 (transient)
2900 < Re (turbulent)

$Re = \frac{\rho v L}{\mu}$

ρ:$fluid\ density\ (\frac{kg}{m^3})$,

v:$fluid\ speed\ \left(\frac{m}{s}\right)$,

L:$Restrictive\ Length/\ tube\ diameter\ (m)$,

μ:$dynamic\ vescosity\ \left(\frac{kg}{m.s}\right)$

Based on our calculation:

$\rho\ (semi-water) \cong 1000\ (\frac{kg}{m^3})$,

$v = \frac{flow\ rate}{cross\ section\ area} = \frac{900\ \mu L/min}{25mm\ \times\ 400\ \mu m} = 0.0015\ (m/s)$,

$L = 400\ (\mu m) = 0.0004\ (m)$,

$\mu\ (semi-water)\ @\ 37°C \cong 0.0007\ (\frac{kg}{m.s})$

So, Reynold's Number in our device is:

$Re = \frac{1000\ \times\ 0.0015\ \times\ 0.0004}{0.0007} = 0.857 \ll 2300 \rightarrow laminar$

Although, our device path's height is small (400um), path's width is wide (25mm). So, such designation would help us to use higher flow rate meanwhile benefit from surface tension and still stay in laminar condition.

[1] J. H. Spurk and N. Aksel, *Fluid Mechanics*. Springer International Publishing, 2019.
[2] F. M. White, *Fluid Mechanics*. McGraw-Hill Education, 2016.

Cell simulation modelling:

To model cell polarization simulation by CST software, we used Ref. 20 {in manuscript} [1] parameters as reference:
The parameters are:

	Normal cell	Cancer cell
σ_M: Medium conductivity (S/m)	0.01	0.01
σ_m: Membrane conductivity (S/m)	5.6E-5	9.1E-6
σ_{cyt}: Cytoplasm conductivity (S/m)	1.31	0.48
ε_M: Medium Dielectric constant	80 ε_0	80 ε_0
ε_m: Membrane Dielectric constant	12.8 ε_0	9.8 ε_0
ε_{cyt}: Cytoplasm Dielectric constant	60 ε_0	60 ε_0

DEP (in its simplest form) is due to the interaction of a particle's dipole and the spatial gradient of the electric. One general form of the expression is

$$F_{DEP} = p.\nabla E \qquad \text{[Eq.1]}$$

p is the particle's dipole moment, ∇E is the gradient of the electric field.
For a uniform sphere placed into a sinusoidal electric field given by **E(r,t)** = Re[E(r)e $^{j\omega t}$], where **E(r)** is the complex electric-field phasor that contains spatial information on the field intensity and polarization, the overall induced dipole is given by

$$p(r) = 4\pi\varepsilon_M R^3 \left(\frac{\varepsilon_C - \varepsilon_M}{\varepsilon_C + 2\varepsilon_M}\right) E(r) = 4\pi\varepsilon_M R^3 \cdot K(\omega) \cdot E(r) \qquad \text{[Eq.2]}$$

where R is the radius of the particle; ε_M and ε_C are the complex permittivities of the medium and the cell, respectively, and are each given by $\boldsymbol{\varepsilon} = \varepsilon + \sigma/(j\omega)$, where ε is the permittivity of the medium or cell, σ is the conductivity of the medium or cell, and j is $\sqrt{-1}$. K is known as the Clausius-Mossotti (CM) factor.
In a linearly polarized sinusoidal field, we can combine Equations 1 and 2 to arrive at an expression for the time-average DEP force, given by

$$\langle F_{DEP}(r) \rangle = \pi R^3 Re[K(\omega)].\nabla |E(r)|^2 \qquad \text{[Eq.3]}$$

where ⟨⟩ denotes the time average. If the relative polarizability of the cell is greater than that of the medium, then Re[K(ω)] will be positive (known as positive DEP, or pDEP), and the force will be directed up the field gradient. If the cell is less polarizable than the medium, then Re[K(ω)] is negative, and the force will be directed down the field gradient (negative DEP, or nDEP). Examining the expression for K(ω) in Equation 2, one sees that Re[K(ω)] can only vary between +1 and −0.5.
Of course, cells are neither uniform (e.g., they are multi-layered particles with a membrane, cytoplasm, etc.) nor necessarily spherical (e.g., red blood cells, some bacteria). These complications do not alter the fundamental physics, but rather result in more complicated expressions for the induced dipole (and the resulting DEP force). The complicated internal cellular structure primarily manifests itself in the Clausius-Mossotti factor (K).[2][3]

[1] R. P. Joshi, Q. Hu, K. H. Schoenbach, and S. J. Beebe, "Energy-landscape-model analysis for irreversibility and its pulse-width dependence in cells subjected to a high-intensity ultrashort

electric pulse," *Phys. Rev. E*, vol. 69, no. 5, p. 51901, 2004.
[2] J. Voldman, "Electrical Forces for Microscale Cell Manipulation," *Annu. Rev. Biomed. Eng.*, vol. 8, no. 1, pp. 425–454, 2006.
[3] E. A. Henslee, "Exploiting Clausius-Mossotti Factor to Isolate Stages of Human Breast Cancer Cells: Theory and Experiment." Virginia Tech, 2010.

ANXV/PI Test for viability of the cells exposed to low frequency electric fields

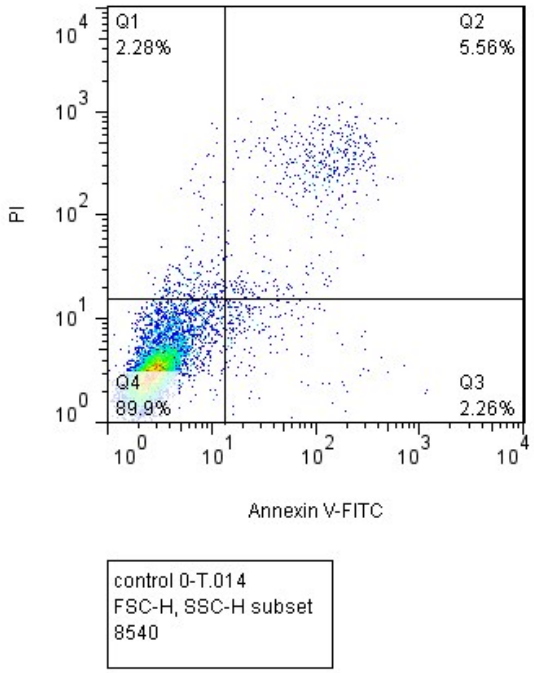

Supplementary Figure 1. Verification of centrifuged cell viability, sample before test. Percentage of viable (Q4), necrotic (Q3), late apoptotic (Q2) and apoptotic (Q1) cells measured by flow citofluorimetry before and after differentiation.

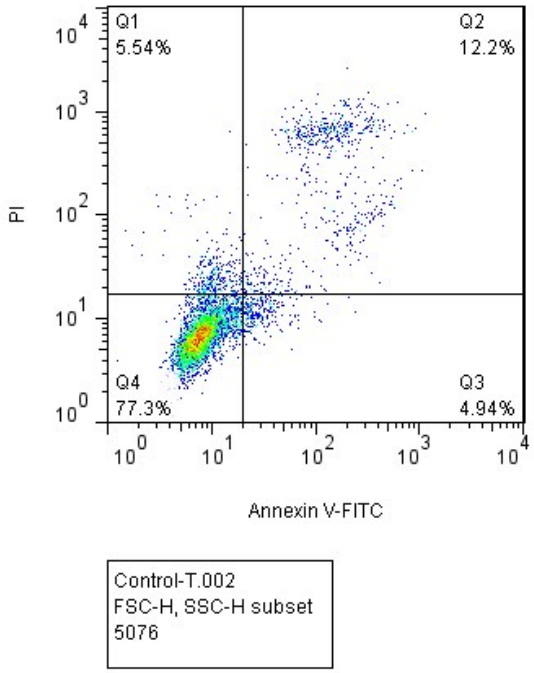

Supplementary Figure 2. Verification of cell viability, sample after test (after stimulation of AC electric field); Percentage of viable (Q4), necrotic (Q3), late apoptotic (Q2) and apoptotic (Q1) cells measured by flow citofluorimetry before and after differentiation.

It is observable that more than 85% of the cells remained alive after stimulation by low frequency AC electric field.

ANXV/PI Description:

To detected cell death, Annexin V/PI double staining kit has been used in flow cytofluorimetric analyses. The Annexin V corresponding signal provides a very sensitive method for detecting cellular apoptosis, while propidium iodide (PI) is used to detect necrotic or late apoptotic cells, characterized by the loss of the integrity of the plasma and nuclear membranes. The data generated by flow cytometry are plotted in two-dimensional dot plots in which PI is represented versus Annexin V-FICT. These plots can be divided in four regions corresponding to:

1) viable cells which are negative to both probes (PI/FITC -/-; Q4);

2) apoptotic cells which are PI negative and Annexin positive (PI/FITC -/+; Q1);

3) late apoptotic cells which are PI and Annexin positive (PI/FITC +/+; Q2);

4) necrotic cells which are PI positive and Annexin negative (PI/FITC +/-; Q3). [1][2][3]

[1] Filograna R, Civiero L, Ferrari V, Codolo G, Greggio E, et al. (2015) Analysis of the Catecholaminergic Phenotype in Human SH-SY5Y and BE(2)-M17 Neuroblastoma Cell Lines upon Differentiation. PLOS ONE 10(8): e0136769.
[2] 1. Kerr JF, Wyllie AH, Currie AR. Apoptosis: a basic biological phenomenon with wide-ranging implications in tissue kinetics. *Br J Cancer*. 1972;26:239-257.
[3] https://www.bdbiosciences.com/documents/BD_FACSVerse_Apoptosis_Detection_AppNote.pdf

Comparison between CTC enrichment methods:
*Be noticed that some methods cannot applicable for cancer or CTC separation based on principle.

Supplementary Table 1. Comparison between cell sorting methods.

Features of the method	Principle	Purity	Recovery	Yield	Efficiency	Cell viability	Sample volume	Throughput (speed)	Ref.
Adherence	Adherence	Low	High	High	Low	High	High	High	1-5
Filtration	Size	Low	High	High	Low	High	High	High	1, 6-9
Centrifugation	Density	Low	High	High	Low	High	High	High	1, 10, 11
Panning	Antibody/ Size	Medium	Medium	Medium	Medium	High	High	High	1, 12-16
MACS	Antibody with Magnetic Beads	High	Medium	Medium	High	High	Medium	Medium	1, 17-20
FACS	Antibody with Fluorescent beads	High	Medium	Low	High	High	Medium	Medium	1, 21-24
LMD	Morphological/ Cytochemical/ Antibody	High	High	Low	Low	No	Small	Low	1
Optical Tweezer	Hydrodynamics	Medium	High	High	Medium	High	Low	Low	25
Acoustophoresis (Not applicable for Cancer)	Hydrodynamics	High	High	High	High	High	High	High	26
EP	Surface Charge	Medium	High	Low	High	Medium	High	High	27, 28
DEP @ Low Frequency	**Polarization/ Dielectric property**	**Medium**	**High**	**Medium**	**High**	**High**	**High**	**High**	**This Paper**
DEP @ High Frequency	Polarization/ Dielectric property	Low	High	Low	High	High	High	Low	29, 30

highlighted advantages of our system Vs. DEP:

- DC-based and low frequency DEP with good consideration of safety (joule thermal increment, solvent electrolysis and cell viability) can be more efficient in cell separation.
- DC-based and low frequency DEP are better choice for external samples like cytological samples which they will be useless after analysis.
- There was lack of studies in low frequencies DEP for cancer detection.
- CPF of cells can be a label-free marker in phenotype sorting.
- It is not essential that CTC detection system only detect CTC in blood which is not an early detection. We believe early CTC diagnosis can be detect in liquid biopsy samples which are a transient level between tumor formation and metastasis.

[1] M. Almeida, A. C. Garc.a-Montero, and A. Orfao, “Cell purification: A new challenge for biobanks,” Pathobiology, vol. 81, pp. 261–275, 2014.
[2] J. A. DeQuach et al., “Simple and High Yielding Method for Preparing Tissue Specific Extracellular Matrix Coatings for Cell Culture,” PLoS One, vol. 5, no. 9, p. e13039, Sep. 2010.
[3] J. Weischenfeldt and B. Porse, “Bone marrow-derived macrophages (BMM): Isolation and applications,” Cold Spring Harb. Protoc., vol. 3, no. 12, pp. 1–7, 2008.
[4] L.-B. Weiswald, D. Bellet, and V. Dangles-Marie, “Spherical cancer models in tumor biology,” Neoplasia, vol. 17, no. 1, pp. 1–15, Jan. 2015.
[5] D. C. Colter, R. Class, C. M. DiGirolamo, and D. J. Prockop, “Rapid expansion of recycling stem cells in cultures of plastic-adherent cells from human bone marrow,” Proc. Natl. Acad. Sci. U. S. A., vol. 97, no. 7, pp. 3213–3218, Mar. 2000.
[6] P. Pinzani et al., “Isolation by size of epithelial tumor cells in peripheral blood of patients with breast cancer: correlation with real-time reverse transcriptasepolymerase chain reaction results and feasibility of molecular analysis by laser microdissection,” Hum. Pathol., vol. 37, no. 6, pp. 711–718, 2006.
[7] Y. Tang, J. Shi, S. Li, L. Wang, Y. E. Cayre, and Y. Chen, “Microfluidic device with integrated microfilter of conical-shaped holes for high efficiency and high purity capture of circulating tumor cells,” Sci. Rep., vol. 4, pp. 1–7, 2014.
[8] L. Pang et al., “Deformability and size-based cancer cell separation using an integrated microfluidic device,” Analyst, vol. 140, no. 21, pp. 7335–7346, 2015.
[9] Y. Yoon et al., “Clogging-free microfluidics for continuous size-based separation of microparticles,” Sci. Rep., vol. 6, no. 1, p. 26531, 2016.
[10] N. Norouzi, H. C. Bhakta, and W. H. Grover, “Sorting cells by their density,” PLoS One, vol. 12, no. 7, p. e0180520, Jul. 2017.
[11] M. Stohr and M. Volm, “Isopycnic Density-Gradient Centrifugation: A Separation Parameter Which Improves Flow Cytometric Measurements on Heterogeneous Tumors,” vol. 149, pp. 141–149, 1983.
[12] “late as m a n y hybridomas as possible , secreting different monoclonal antibodies directed against a variety of antigens . An answer to this problem is a technique in which hybridomas are selected and cloned in one step immediately after fusion , as ,” Animals, vol. 50, pp. 161–171, 1982.
[13] J. P. Beech, S. H. Holm, K. Adolfsson, and J. O. Tegenfeldt, “Sorting cells by size, shape and deformability,” Lab Chip, vol. 12, no. 6, pp. 1048–1051, 2012.
[14] P. Preira, V. Grandné, J.-M. Forel, S. Gabriele, M. Camara, and O. Theodoly, “Passive circulating cell sorting by deformability using a microfluidic gradual filter,” Lab Chip, vol. 13, no. 1, pp. 161–170, 2013.
[15] W. Beattie, X. Qin, L. Wang, and H. Ma, “Clog-free cell filtration using resettable cell traps,” Lab Chip, vol. 14, no. 15, pp. 2657–2665, 2014.
[16] S. M. McFaul, B. K. Lin, and H. Ma, “Cell separation based on size and deformability using microfluidic funnel ratchets,” Lab Chip, vol. 12, no. 13, pp. 2369–2376, 2012.
[17] S. Miltenyi, W. Müller, W. Weichel, and A. Radbruch, “High gradient magnetic cell separation with MACS.,” Cytometry, vol. 11, no. 2, pp. 231–238, 1990.
[18] H. Xu et al., “Antibody conjugated magnetic iron oxide nanoparticles for cancer cell separation in fresh whole blood,” Biomaterials, vol. 32, no. 36, pp. 9758– 9765, Dec. 2011.
[19] K. E. McCloskey, J. J. Chalmers, and M. Zborowski, “Magnetic cell separation: characterization of magnetophoretic mobility.,” Anal. Chem., vol. 75, no. 24, pp. 6868–6874, Dec. 2003.
[20] G. Blankenstein, “Microfabricated Flow System for Magnetic Cell and Particle Separation BT - Scientific and Clinical Applications of Magnetic Carriers,” U. Häfeli, W. Schütt, J. Teller, and M. Zborowski, Eds. Boston, MA: Springer US, 1997, pp. 233–245.
[21] W. A. Bonner, H. R. Hulett, R. G. Sweet, and L. A. Herzenberg, “Fluorescence activated cell sorting.,” Rev. Sci. Instrum., vol. 43, no. 3, pp. 404–409, Mar. 1972.
[22] M. Brown and C. Wittwer, “Flow cytometry: principles and clinical applications in hematology.,” Clin. Chem., vol. 46, no. 8 Pt 2, pp. 1221–1229, Aug. 2000.
[23] S. Nagrath et al., “Isolation of rare circulating tumour cells in cancer patients bymicrochip technology,” Nature, vol. 450, p. 1235, Dec. 2007.
[24] P. T. H. Went et al., “Frequent EpCam protein expression in human carcinomas,” Hum. Pathol., vol. 35, no. 1, pp. 122–128, 2004.
[25] X. Wang et al., “Enhanced cell sorting and manipulation with combined optical tweezer and microfluidic chip technologies.,” Lab Chip, vol. 11, no. 21, pp. 3656– 3662, Nov. 2011.
[26] Mengxi Wu, et al., “Acoustofluidic exosome isolation from whole blood”, Proceedings of the National Academy of Sciences Oct 2017, 114 (40) 10584-10589.

[27] B. Chen et al., “Targeting negative surface charges of cancer cells by multifunctional nanoprobes,” Theranostics, vol. 6, no. 11, pp. 1887–1898, 2016.
[28] M. Jahangiri et al., “Microfluidic platform with integrated electrical actuator to enrich and locating atypical/cancer cells from liquid cytology samples," Sensors and Actuators B: Chemical, vol. 297, p. 126733, 2019
[29] x Tada, Shigeru et al. “High-throughput separation of cells by dielectrophoresis enhanced with 3D gradient AC electric field.” Biomicrofluidics vol. 11,6 064110. 13 Dec. 2017.
[30] Hadady, Hanieh et al. “High frequency dielectrophoretic response of microalgae over time.” Electrophoresis vol. 35,24 (2014): 3533-40.